ELSEVIER

Review

Heat and Flow Characteristics of Packed Beds

E. Achenbach
Institute of Energy Process Engineering, Jülich, Germany

■ The state of the art is presented for the heat and flow characteristics of packed beds under conditions where radiant heat transfer may be neglected. Equations for the prediction of convective heat transfer, pressure drop, effective thermal conductivity, and wall heat transfer are recommended. New experimental data of heat transfer and pressure drop that exceed the previous Reynolds number range by one order of magnitude up to $\mathrm{Re}/\epsilon = 7.7 \times 10^5$ are reported. Sources of errors that may occur during experimental work are discussed and partly quantified.

Keywords: *packed beds, pressure drop correlations, convective heat transfer, effective thermal conductivity*

INTRODUCTION

The importance of research in the field of porous media may be demonstrated by the large number of publications on the subject, about 150 per year. The domain of application is wide spread, ranging from catalytical and chemical particle beds, mass separator units, and heat exchangers to thermal insulation, debris beds, soil investigations (oil recovery), heat pipes, and fluidized beds. About one fourth of the work is devoted to fluidized beds including immersed bodies, one-third deals with natural convection in saturated porous media, another fourth with heat and mass transfer problems under forced convection, and about one-tenth treat the field of effective conductivity.

The basic idea for the treatment of particle-to-fluid heat transfer in porous media is to consider the situation for the individual particle. Appropriate quantities for the length scale and the velocity, together with a geometrical function, are sufficient to correlate the results of the single particle with those of the packing [1]. These characteristic quantities must combine the statistical parameter of the porous medium, that is, the porosity, with characteristic quantities that are easily accessible, for instance, particle size and mean fluid velocity.

The pressure drop is calculated from equations initially established for channel flow. To apply them to porous media, the same characteristic quantities must be introduced. Doing so for laminar flow, encounters the so-called Darcian flow, which is characterized by a linear relationship between pressure drop and mass flow. In many situations, particularly when natural convection occurs, the conditions of Darcian flow prevail. This is true for local Reynolds numbers $\mathrm{Re} < 1$. Beyond this threshold, inertial effects may play an increasing role.

The major concept when treating the problem of effective conductivity is that of the cell model proposed by Zehner and Schlünder [2]. In this model a characteristic unit cell is cut out representing the solid and fluid phase situation in the bed. In this unit cell the particular heat-transferring mechanisms are considered.

The present paper presents the state of the art with regard to heat transfer, pressure drop, effective conductivity, and wall heat transfer for particulate beds of nonuniform porosity. Emphasis is given to spherical particles. Because of the large field of research treated, only more recent or earlier basic contributions are cited. Fuller information is to be found in the cited review papers.

FLOW AND HEAT TRANSFER CHARACTERISTICS

The statistical quantity of a randomly packed bed is the void fraction ϵ, which is defined as

$$\epsilon = 1 - \frac{V_s}{V_t}, \tag{1}$$

where V_s is the volume of the solid particles and V_t the total volume.

The length scale, that is, the hydraulic diameter of the system, is dependent on the void fraction and the pebble diameter d:

$$d_h = d\frac{\epsilon}{1-\epsilon}. \tag{2}$$

The mean pore velocity correlates with ϵ and with the mean velocity u in the empty tube,

$$u_p = u/\epsilon. \tag{3}$$

Address correspondence to Dr.-Ing. E. Achenbach, Institute of Energy Process Engineering (IEV), Research Center Jülich (KFA), D-52425 Jülich, Germany.

Experimental Thermal and Fluid Science 1995; 10:17–27

655 Avenue of the Americas, New York, NY 10010

0894-1777/95/$9.50
SSDI 0894-1777(94)00077-L

Thus we obtain for the Reynolds number

$$\mathrm{Re}_h = \frac{d_h u_p \rho}{\eta} = \frac{1}{1-\epsilon}\mathrm{Re}, \tag{4}$$

where

$$\mathrm{Re} = \frac{ud\rho}{\eta}, \tag{5}$$

and for the Nusselt number

$$\mathrm{Nu}_h = \frac{\alpha d_h}{\lambda} = \mathrm{Nu}\frac{\epsilon}{1-\epsilon}, \tag{6}$$

where

$$\mathrm{Nu} = \alpha d/\lambda. \tag{7}$$

Assuming that the heat transfer from pebble beds can be expressed in terms of the function

$$\mathrm{Nu}_h = f(\mathrm{Re}_h; \mathrm{Pr}), \tag{8}$$

empirical heat transfer results will obey the equation

$$\mathrm{Nu} = \frac{1-\epsilon}{\epsilon} f\left(\frac{\mathrm{Re}}{1-\epsilon}; \mathrm{Pr}\right). \tag{9}$$

Defining the pressure drop coefficient as

$$\Psi = \frac{\Delta p}{(H/d_h)(\rho/2)u_p^2}, \tag{10}$$

where H is the total height of the packing, this quantity becomes

$$\Psi = \frac{\Delta p}{(H/d)(\rho/2)u^2}\left(\frac{\epsilon^3}{1-\epsilon}\right), \tag{11}$$

with d_h and u_p from Eqs. (2) and (3).

The pressure drop coefficient Ψ is a function of Reynolds number Re_h,

$$\Psi = f(\mathrm{Re}_h) = f\left(\frac{\mathrm{Re}}{1-\epsilon}\right). \tag{12}$$

FORCED CONVECTIVE HEAT TRANSFER

The forced convective heat transfer is influenced by a number of parameters, for instance, Reynolds number, Prandtl number, void fraction, ratio of tube diameter to sphere diameter, ratio of bed height to sphere diameter, local flow conditions, effects of radiation, contact conduction, natural convection, and surface roughness. This is the reason the experimental results found in the literature show considerable departures from one another. Many of the more than 100 papers in this field therefore report on results under certain conditions and cannot be generalized to represent the convective heat transfer in an "infinitely" large randomly packed bed. In particular, the void fraction and the ratio of tube to sphere diameter are parameters of strong influence, which has often not been recognized. Therefore many authors do not report on the corresponding details, which makes an evaluation of the results impossible. The present paper addresses the effect of some of the parameters mentioned above and quantifies their importance.

The measurement techniques applied for pebble bed heat transfer are

- Heat transfer from an electrically heated single sphere buried in the unheated packing
- Mass transfer tests making use of the analogy between heat and mass transfer
- Simultaneous heat and mass transfer
- Regenerative heating
- Semiempirical methods

The method of the single heated sphere requires that the gas mixing downstream of the particle is nearly perfect. If this is true, this technique is very simple and accurate. The heating rate and the temperature difference between the wall and the bulk can easily be determined. Using copper or brass for the probe material, the boundary condition of constant surface temperature is approximately obtained. Radiation can be minimized by using highly polished surfaces. To avoid uncontrolled heat losses via the points of contact with the unheated neighboring spheres, the thermal conductivity of those neutral spheres should be low compared to that of the active probe.

Mass transfer experiments with single spheres are preferably conducted according to the method of naphthalene sublimation in air. This makes use of the weight loss of naphthalene due to sublimation during a time interval Δt. It promises to be a very successful way of producing reliable results. The boundary condition is constant wall concentration, corresponding to constant wall temperature in heat transfer experiments.

Effects of heat radiation and contact heat conduction cannot occur, and the effect of natural convection, which becomes relevant at low Reynolds numbers, is essentially reduced, as the Grashof number is lower by three orders of magnitude than in heat transfer experiments. A crucial point is the strong dependence of the naphthalene vapor pressure on the temperature, which requires a very exact wall temperature measurement. An error of 1°C causes an error of 10% in the determination of the mass transfer coefficient. A further disadvantage is the noncontinuous nature of the technique, which requires the preparation of new naphthalene test spheres for each particular Reynolds number run.

Some authors apply the method of simultaneous heat and mass transfer. Porous particles are saturated with a fluid that evaporates during the test run. The temperature decrease and the weight loss of the spheres can be evaluated separately in terms of the heat transfer coefficient. This method is not so easy to handle, and difficulties arise in determining the exact surface temperature, which is strongly affected by the evaporation process.

The regenerative heating technique is based on unsteady heat transfer from a pebble bed. Appropriate heating and cooling of the packing leads to temperature profiles that can be evaluated in terms of the heat transfer coefficient. This method requires significant technical and mathematical effort.

The semiempirical methods start from a hypothesis as the basis for the derivation of empirical relationships. The heat transfer from a pebble bed, for instance, can be related to the heat transfer for a single sphere. The adjustment to experimental results is then done by means of geometrical parameters.

A very successful application of a semiempirical method is that published by Gnielinski [1]. The method is based on the idea that the heat transfer from arbitrary particles can be predicted by applying the equations for a flat plate if a suitable length scale and velocity are introduced. This characteristic length scale is the distance traveled by a fluid particle on its way along the body. For spherical particles this length scale is equal to the sphere diameter. The characteristic velocity is the mean velocity in the pores as defined in Eq. (3). Both quantities are introduced into the asymptotic solutions for laminar and turbulent heat transfer,

$$\mathrm{Nu}_1 = 0.664\mathrm{Pr}^{1/3}(\mathrm{Re}/\epsilon)^{1/2} \tag{13}$$

and

$$\mathrm{Nu}_t = \frac{0.037(\mathrm{Re}/\epsilon)^{0.8}\mathrm{Pr}}{1 + 2.443(\mathrm{Re}/\epsilon)^{-0.1}(\mathrm{Pr}^{2/3} - 1)}. \tag{14}$$

The combination of the two asymptotic solutions,

$$\mathrm{Nu}_{sp} = 2 + (\mathrm{Nu}_l^2 + \mathrm{Nu}_t^2)^{1/2}, \tag{15}$$

yields the heat transfer from a single sphere. The 2 in Eq. (15) is the asymptotic solution for $\mathrm{Re} \to 0$.

Equation (15) can now be applied to pebble beds by defining an empirical arrangement factor $f(\epsilon)$,

$$f(\epsilon) = 1 + 1.5(1 - \epsilon). \tag{16}$$

Thus we find

$$\mathrm{Nu} = f(\epsilon)\,\mathrm{Nu}_{sp}. \tag{17}$$

The set of Eqs. (13)–(17) is suitable for correlating the experimental results up to high Reynolds numbers for void fractions in the range $0.26 < \epsilon < 0.935$ and the Prandtl or Schmidt number from 0.7 to 10^4, respectively.

Equation (17) was experimentally covered up to $\mathrm{Re}/\epsilon = 2 \times 10^4$ when [1] appeared. In the present work this range was exceeded by more than one order of magnitude up to $\mathrm{Re}/\epsilon = 7.7 \times 10^5$. The tests were performed in a wind tunnel that was operated with a system pressure up to 40 bar. The fluid was air or helium. Thus the same Reynolds number could be reached by varying the pressure, the mass flow, or the kind of fluid.

The majority of the present experiments were conducted using a bed diameter of $D = 0.983$ m and a bed height of $H = 0.84$ m. To eliminate wall effects, the core wall was structured such that a regular orientation of the spheres adjacent to the wall was avoided. The sphere diameter was $d = 0.06$ m. The void fraction was experimentally determined to be $\epsilon = 0.387$. The heat transfer experiments were carried out by applying the method of the electrically heated single sphere in an unheated packing. The test spheres were manufactured from copper, the surface being highly polished and covered with a silver layer to keep the contribution of thermal radiation low. The remainder of the spheres were graphite except for those in contact with the test sphere. Those spheres were made of acrylic to avoid heat losses via the contact points.

To cover the lower range of Reynolds numbers down to unity ($1 < \mathrm{Re}/\epsilon < 2.5 \times 10^4$), mass transfer experiments were carried out, applying the method of naphthalene sublimation in air. This method was favored to avoid the problems of radiation, natural convection, and contact conduction that occur in heat transfer experiments. Two test installations were used. In addition to the one mentioned above, a bed diameter $D = 0.3$ m and a sphere diameter of $d = 8 \times 10^{-3}$ m were applied. The mass transfer tests were conducted as follows. Spheres covered with a naphthalene layer about 0.5 mm thick were buried in the core for each run. Then the test was started, keeping the gas temperature and the mass flow of the fluid constant. After an appropriate time interval Δt, which had to be adjusted to the magnitude of the mass transfer coefficient β, the loss of naphthalene from the sphere surface was determined. The mass transfer coefficient was then calculated from the mass flux $\dot{m}$ and the partial pressure difference, $p_w - p_\infty$, between the wall and the bulk, where p_∞ was assumed to be zero. This procedure must be repeated for each Reynolds number.

Figure 1 exhibits the present heat and mass transfer results together with those from the semiempirical equation (17). For $\mathrm{Re} > 500$, the experimental results can very well be represented by that relationship. For evaluation of the mass transfer results, with a Schmidt number of $\mathrm{Sc} = 2.5$ it was assumed that the effect of Sc on the Sherwood number can be described by $f(\mathrm{Sc}) = \mathrm{Sc}^{1/3}$.

For Reynolds numbers $\mathrm{Re} < 500$ the present results are lower than those predicted by Gnielinski's formula. This fact was observed and discussed in 1967 by Kunii and Suzuki [3]. Schlünder [4] and Martin [5] tried to explain this evidence by pointing out the effect of the nonuniform void fraction distribution across the bed. If, in this case, the heat transfer coefficient is calculated by means of the overall heat removal from the bed, a cold bypass stream occurs, which indicates a lower heat transfer coefficient than there actually is.

Vortmeyer [6] also comments on the apparent decrease in convective particle–gas heat transfer at low Reynolds numbers. He shows that for $\mathrm{Re} < 200$ the axial dispersion term increasingly dominates the heat transfer. Similar conclusions are drawn by Tsotsas [7] for the situation of particle-to-gas mass transfer.

The present tests were carried out with a single naphthalene-covered sphere in an inert bed. The wall was structured to avoid near-wall bypass effects. Under these conditions Schlünder's hypothesis cannot explain the decreasing trend of the mass transfer. The present measurement technique, however, violates the hypothesis of considering the bed as an arrangement of heated channels of a certain hydraulic diameter. This is true only if all particles are "heated." In this case the boundary layer thickness is restricted to the geometry of the channels and the Nusselt number becomes constant. In the present case for the single mass transfer sphere, the thickness of the boundary layer is not limited and may exceed the channel hydraulic diameter, leading to a continuous decrease in the mass transfer coefficient with decreasing Reynolds number.

Experimental results for convective heat transfer may also be affected by other heat transfer mechanisms. Applying the measurement technique of the separately heated sphere, the influence of radiation can be estimated by assuming radiant heat transfer from a gray body to a black surround, with the temperatures in both locations known by measurement. Furthermore, the results may be checked by means of mass transfer tests. For design purposes,

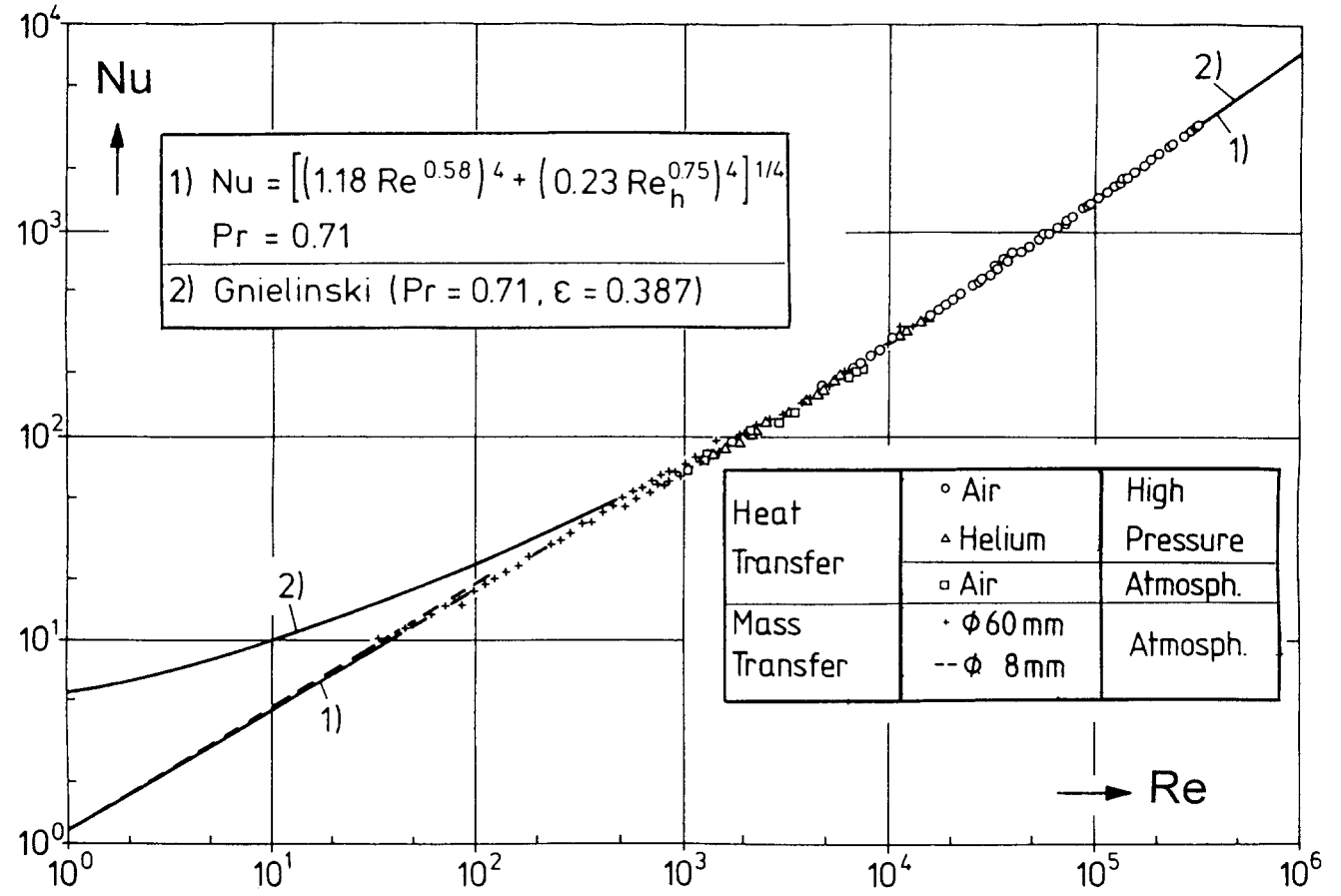

Figure 1. Convective particle-to-fluid heat transfer for pebble beds: (1) Present results; (2) Eq. (17), Pr = 0.7, $\epsilon = 0.387$.

however, the prediction of the radiant heat rate is more complicated and requires a numerical treatment making use of the effective conductivity.

The heat losses via points of contact are a severe problem for the single-sphere method. Figure 2 demonstrates what happens when a copper test sphere is in contact with unheated graphite spheres. The solid line represents the expected result. Over the whole range the heat conducted through the points of contact represents a considerable contribution to the total heat rate. This demonstrates that the spheres surrounding a test sphere must be of low thermal conductivity.

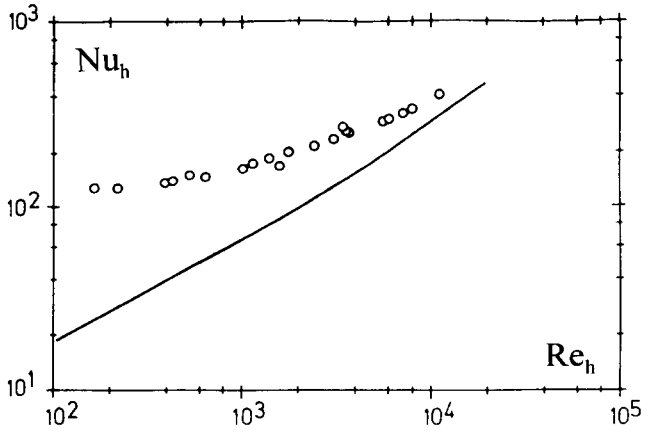

Figure 2. Effect of heat conduction via points of contact.

A further source of error is natural convection, which may occur to augment flow or counter flow. Karabelas et al. [8] correlate their mass transfer results carried out in the Rayleigh number range $1.24 \times 10^7 < \mathrm{Ra} < 3.24 \times 10^9$ by the equations

$$\mathrm{Sh} = 0.46(\mathrm{Gr}\,\mathrm{Sc})^{1/4} \tag{18}$$

for $\mathrm{Ra} = (\mathrm{Gr} \times \mathrm{Sc}) < 10^9$ and

$$\mathrm{Sh} = 0.12(\mathrm{Gr}\,\mathrm{Sc})^{1/3} \tag{19}$$

for $\mathrm{Ra} = (\mathrm{Gr}\ \mathrm{Sc}) > 10^9$, where the Grashof number is defined as

$$\mathrm{Gr} = \frac{gd^3}{\nu^2}\left(\frac{\Delta\rho}{\rho}\right).$$

Equations (18) and (19) can also be applied to heat transfer by replacing the Schmidt number Sc by the Prandtl number and $\Delta\rho/\rho$ by $\Delta T/T_\infty$. Our own heat and mass transfer results, obtained in the lower range of Rayleigh numbers, $5 < \mathrm{Ra} < 5 \times 10^6$ and with variable void fraction, confirm Eq. (18). Furthermore, the present results indicate that within the scatter of the results the natural convective heat/mass transfer is independent of the void

fraction ϵ (Fig. 3). It can be correlated with the relation valid for the single sphere (Eq. 20) given by [9],

$$\mathrm{Nu} = 2 + 0.56\left(\frac{\mathrm{Pr}}{0.846 + \mathrm{Pr}}\mathrm{Ra}\right)^{1/4}. \qquad (20)$$

Figure 4 gives an example of heat transfer measurements with convective counterflow. The data points level out to a constant value that corresponds to the natural convective heat transfer.

The method of the single heated sphere requires knowledge about the statistics of local heat transfer in the bed. For this purpose heat transfer experiments were carried out at four Reynolds numbers in the range $10^4 < \mathrm{Re} < 10^5$ by burying the test spheres in different random positions in the bed. The measurement made from each of the 20 tests yields a standard deviation of $\sigma < 5\%$ independent of Re. The maximum deviation was $+7.3\%$ and -10.6%. These data refer to the interior of a bed, the wall of which was structured to avoid bypass effects.

The heat transfer from spheres positioned in the entrance layer of a bed is expected to be lower than the average value because the velocity and the turbulence level of the incident flow are smaller than the superficial velocity. Figure 5 exhibits this comparison. The difference seems to decrease for low Reynolds numbers.

PRESSURE DROP COEFFICIENT

The experimental work on pressure drop through packed beds shows a large scatter in the results. This is with a view to Eq. (11), predominantly due to the essential effect the void fraction ϵ has on the pressure loss. In most of the numerous papers evaluated in [10], the void fraction ϵ was not determined exactly enough or not at all. Thus only a few relevant papers were left whose results can be approximated by

$$\Psi = \frac{320}{\mathrm{Re}/(1-\epsilon)} + \frac{6}{[\mathrm{Re}/(1-\epsilon)]^{0.1}}. \qquad (21)$$

Equation (21) is confirmed by experimental results up to $\mathrm{Re}/(1-\epsilon) = 5 \times 10^4$. Further tests in a high-pressure wind tunnel applied for the present work permitted this range to be extended by about one order of magnitude. These results indicate that for $\mathrm{Re}/(1-\epsilon) > 10^5$ the pressure drop coefficient seems to become independent of Re (Fig. 6). Therefore, Eq. (21) only holds for $\mathrm{Re}/(1-\epsilon) \leq 10^5$.

The first term of Eq. (21) represents the asymptotic solution for the laminar flow, the second term, the solution for turbulent flow. Each of the terms can be written as

$$\Psi = A\left(\frac{\mathrm{Re}}{1-\epsilon}\right)^{-n} = A(1-\epsilon)^n \mathrm{Re}^{-n}, \qquad (22)$$

where $n = 1$ represents the low Re range and $n = 0.1$ the high one. The sensitivity of Eq. (21) to the influence of ϵ can be pointed out by writing

$$\frac{d(\Delta p)}{\Delta p} = \frac{\partial(\Delta p)}{\partial \epsilon}\frac{d\epsilon}{\Delta p}. \qquad (23)$$

Equations (11) and (22), together with Eq. (23), yield

$$\frac{d(\Delta p)}{\Delta p} = -\frac{3 - \epsilon(2-n)}{1-\epsilon}\frac{d\epsilon}{\epsilon}. \qquad (24)$$

A positive relative variation of ϵ causes a negative variation in the pressure drop multiplied by a factor that is dependent on the void fraction ϵ and on the slope n of the Reynolds number (see also Fig. 7). At $\epsilon = 0.4$, for instance, an error of 1% in ϵ causes an error of 4% for Δp.

BYPASS EFFECT

The strong dependence of the pressure drop on the void fraction causes a nonuniform velocity distribution across the particle bed, since the disturbance of the statistical particle arrangement adjacent to the wall generates here a higher void fraction than the average value in the bed. For spherical particles, Benenati and Brosilow [11], Goodling and Vachon [12], and Ouchlyama and Tanaka [13] mea-

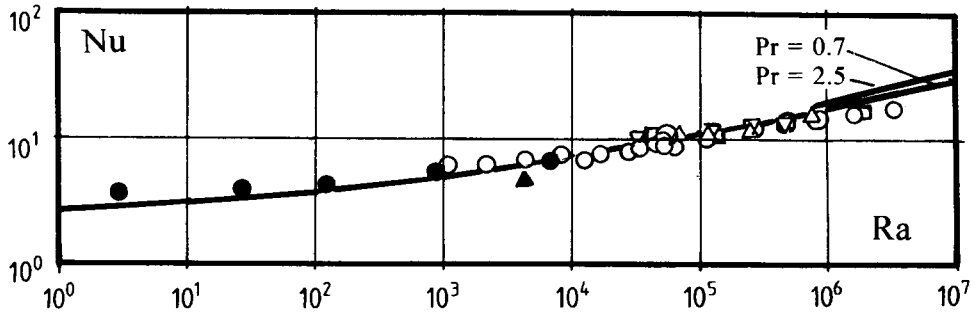

ε	1.0	0.476	0.302	0.26
heat	○	△	□	▽
mass	●	▲	–	–

Figure 3. Natural convective heat/mass transfer in pebble beds; solid lines: Eq. (20).

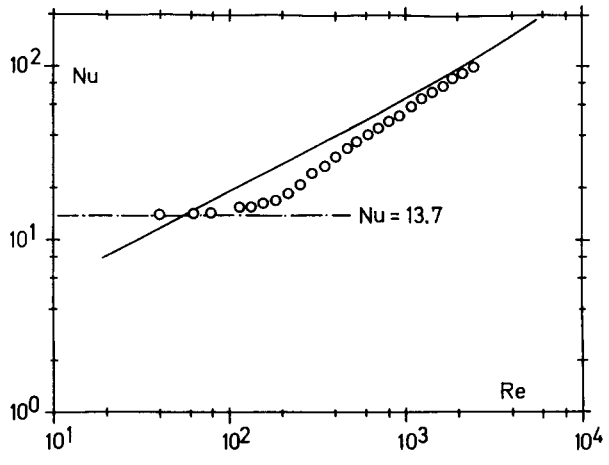

Figure 4. Mixed convective heat transfer in pebble beds under opposing flow conditions.

sured the radial void fraction distribution as shown in Fig. 8. The void fraction ϵ decreases from unity at the wall to a minimum of $\epsilon = 0.2$ at a distance of $d/2$ and then levels out with decreasing amplitudes to a constant value. This point is reached at a distance of nearly four sphere diameters from the wall. Recently Daszkowski [14] determined also the axial void fraction distribution in spherical beds, starting both from the free surface of the bed and from the bottom plate (Figs. 9 and 10).

Similar experiments on void fraction distribution have been conducted also for other particle shapes used in catalyst techniques. Raschig rings and full cylinders have been investigated by Roblee et al. [15] (Fig. 11). Figure 11 represents also our own results [16] for the hollow cylinder with a diameter ratio of $d_i/d_a = 0.425$. Thin-walled rings show an effect only for a wall distance of $r < 1d$. Full cylinders vary with a wavelength of $1d$ and thick-walled cylinders with $d/2$ as an effect of the inner voidage of the particle.

The radial variation of the void fraction has this effect of generating a near-wall bypass flow. The higher velocities near the wall are not only of importance for the local

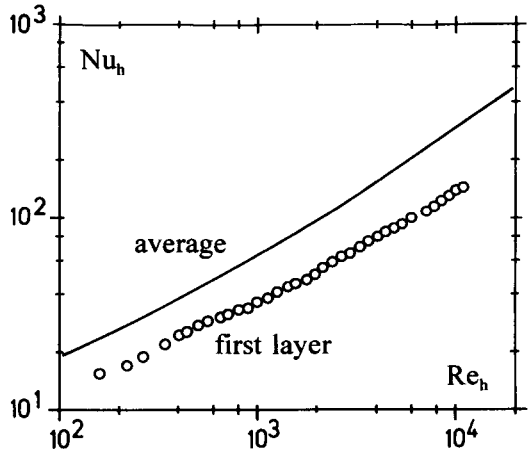

Figure 5. Convective heat transfer in the entrance region of a pebble bed.

flow, heat, and mass transfer in this region but also influence integral quantities of the packing such as the total pressure drop and heat/mass transfer. Therefore numerous authors have measured or calculated the velocity distribution across the bed. A comprehensive review in this field was published in [17]. Recent experimental and computational results are also to be found in [14].

As mentioned above, it can be demonstrated that the effect of bypass flow is the main reason for the severe departures of experimental pressure drop results. The higher the ratio of sphere to tube diameter, d/D, the stronger is the influence on the pressure drop. This can easily be shown when assuming, for a rough estimation, that the bed is subdivided into a near-wall region (index w) and a central region (index c). The corresponding void fractions required for the calculation can be obtained by evaluating the experimental results for the overall value from Carman [18] and Barthels [19],

$$\epsilon = 0.78(d/D)^2 + 0.375, \tag{25}$$

and for the wall value from [10],

$$\epsilon_w = 63.6\left(\frac{D}{d} + 15\right)^{-2} + 0.43. \tag{26}$$

The central void fraction can then be calculated from

$$\epsilon_c = \epsilon_w - \frac{\epsilon_w - \epsilon}{(1 - d/D)^2}. \tag{27}$$

The velocity ratios wall-to-center, u_w/u_c, and center-to-average, u_c/u, can be determined by means of the pressure drop equation (11). The result is shown in Fig. 12. With increasing ratio d/D the wall effect becomes more and more important.

When evaluating experiments on pressure drop without accounting for the bypass effect, the mean velocity calculated from the mass flow is higher than the actual central velocity. Therefore the pressure drop coefficient evaluated with the mean velocity is too low. This effect is exhibited in Fig. 13, which shows the ratio of apparent to exact pressure drop coefficient. At $d/D = 0.2$, for instance, the error is about 28%. The reliability of experimental pressure drop results therefore decreases with increasing ratio d/D unless a correction for the bypass has been made.

THERMAL CONDUCTIVITY

The thermal conductivity of a packed bed is no longer merely a material property but depends also on the flow and heat transfer conditions and on the size and shape of the particles. Therefore it is called the effective thermal conductivity, λ_e, which means that the bed is considered a quasi-continuum and the conductive heat flux q can be calculated by means of the Fourier equation.

The thermal conductivity is separated into two contributions: the stagnant gas conductivity, λ_0, and the conductivity due to macroscopic flow effects, λ_k, where

$$\lambda_e = \lambda_0 + \lambda_k. \tag{28}$$

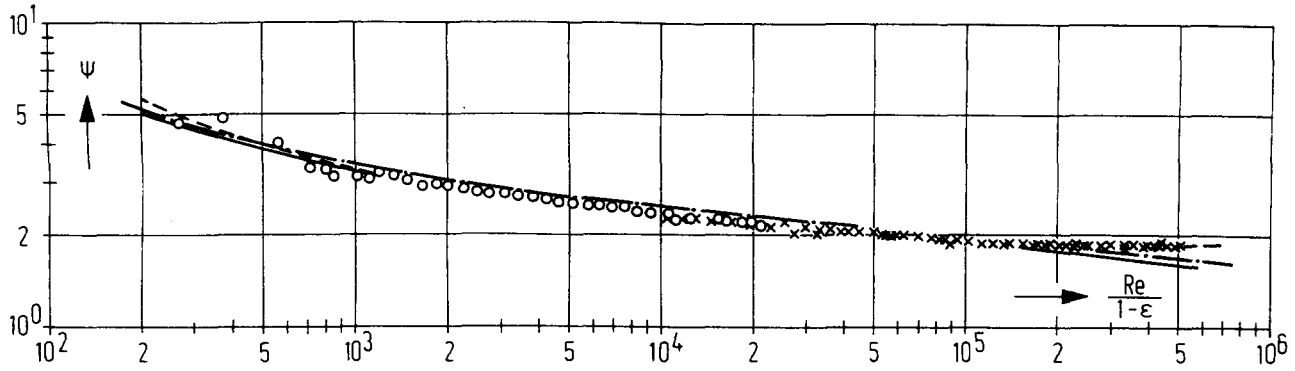

Figure 6. Pressure drop coefficient of pebble beds. (×) High pressure, (○) ambient pressure. —— Eq. (21), —·— ref. [22].

The latter quantity accounts for the dispersion due to the flow and is therefore related to the Peclet number (Pe). The relation given by Yagi et al. [20],

$$\frac{\lambda_k}{\lambda_g} = \frac{\mathrm{Pe}}{K}, \tag{29}$$

is well established and linearly correlates the dispersion term with the Peclet number. The quantity K is different for radial and axial conductivity and is dependent on the geometrical conditions of the packing. For the radial case and spherical particles, experimental results have been correlated by Schlünder [21],

$$K_r = 8\left[2 - \left(1 - 2\frac{d}{D}\right)^2\right]. \tag{30}$$

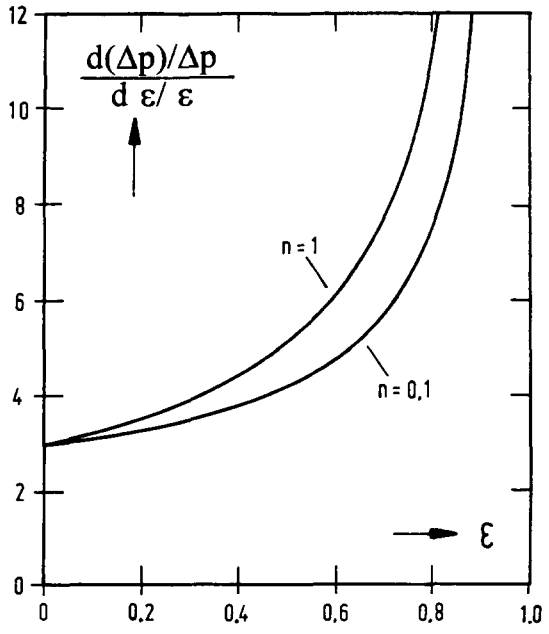

Figure 7. Sensitivity of the pressure drop to changes in the void fraction.

The corresponding value for the axial conductivity is reported [6, 21] to be $K_{ax} = 2$. Data for other particle shapes are also found in the VDI-Wärmeatlas [22].

The constant K_r in Eq. (30), which is equal to 8 for spherical infinite beds, can be understood as the turbulent Peclet number of the system. It describes the heat exchange due to the velocity fluctuations, which are independent of the Reynolds number to a first approximation. Thus Pe/K is the ratio of turbulent to molecular heat conductivity.

The stagnant gas effective conductivity, λ_0, is influenced by several heat transfer mechanisms: (1) conduction through the gaseous phase, (2) conduction through the solid phase, (3) heat radiation solid–solid and through the void area to the next layer, (4) conduction through the contact area, and (5) pressure-dependent conductivity caused by the Smoluchowski effect.

Tsotsas and Martin [23, 24] have carried out a comprehensive review of the thermal conductivity of packed beds. They comment on the numerous models for the determination of λ_e. The most advanced model is the Zehner-Bauer-Schlünder model [25–28], which accounts for all effects mentioned above. Therefore it is recommended in the VDI-Wärmeatlas [22] for engineers' application. The idea of that model is to cut out a unit cell and consider

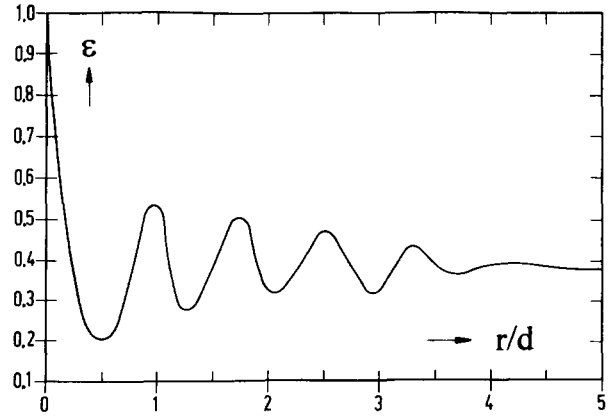

Figure 8. Radial void fraction distribution. (After Ref. 11.)

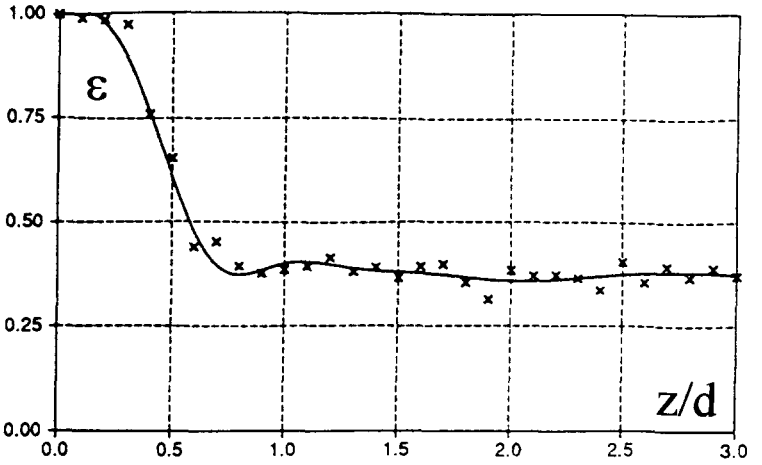

Figure 9. Axial void fraction distribution measured from the free sphere layer of the bed. (After Ref. 14.)

the heat flux assuming parallel heat flux vectors. The set of equations that are applicable to various shapes of particles and also to binary systems is voluminous. It will not be repeated in this paper but can be found in [22].

The paper by Dalle Donne and Sordon [29] theoretically and experimentally treats the thermal conductivity of beds consisting of particles of different sizes and different solid conductivities. The authors apply the Zehner-Bauer-Schlünder model mentioned above and a model by Okasaki et al. [30] established for binary particle mixtures. After modifications they were able to correlate their experimental results with satisfactory accuracy.

Botterill et al. [31] investigated the effective thermal conductivity of particulate beds for small particles (alumina 376 μm; sand 410 and 590 μm) at high temperatures (400–950°C). In their analysis in [32], these authors reviewed several models and found that none of them could predict the strong temperature dependence of the effective conductivity. They assume that the reason for this evidence is that the material is partly transmissive.

Finally, excellent experimental results by Robold [33], which have not been noticed in the literature, should be reported on. He measured the conductivity of a closely sized bed of spherical particles up to 1870 K in vacuum and in helium using either high-conductive spheres of graphite or low-conductive spheres of ZrO_2. The experimental results are in good agreement with his theory, which is a modification of the Zehner-Bauer-Schlünder model (Fig. 14). The dashed line represents the result for stagnant helium according to [22], which overpredicts the experimental data in the lower range of temperature. With increasing temperature the agreement improves, which means that the radiation through the pores is correctly modeled. The decreasing slope of the curve for $T > 1400$ K results from the diminution of the graphite conductivity with increasing temperature.

WALL-TO-FLUID HEAT TRANSFER

In many technical applications a heat flux penetrates the wall of the packed bed in order to heat it, to cool it, or to supply a chemical reaction. In this situation the heat has to pass the wall boundary layer established by the streaming fluid. Its thickness depends on the Reynolds and Prandtl numbers and generally is small compared to the particle size. Similarly a thermal boundary layer exists that causes a temperature difference $\Delta\vartheta$ across this region. The heat flux at the wall, q_w, can be expressed by Newton's law,

$$q_w = \alpha_w \Delta\vartheta, \tag{31}$$

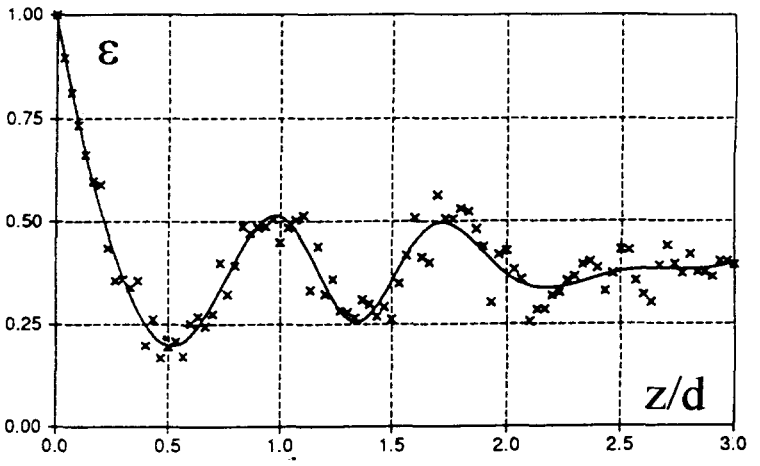

Figure 10. Axial void fraction distribution measured from the bottom plate. (After Ref. 14.)

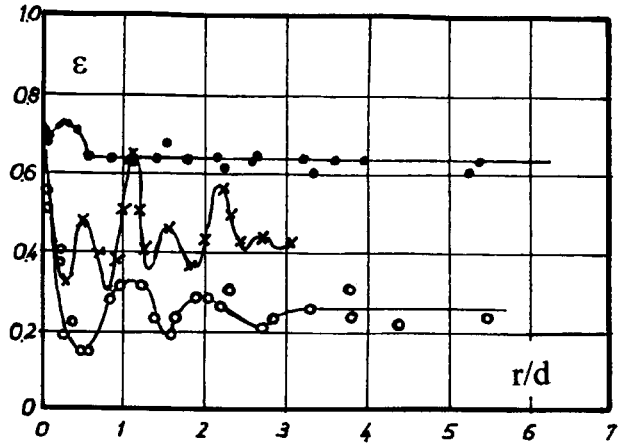

Figure 11. Radial void fraction distribution. Ref. 14: ring (○), d_i/d_a = 0.67–0.77; full cylinder (●). Ref. 16: ring (×), d_i/d_a = 0.425.

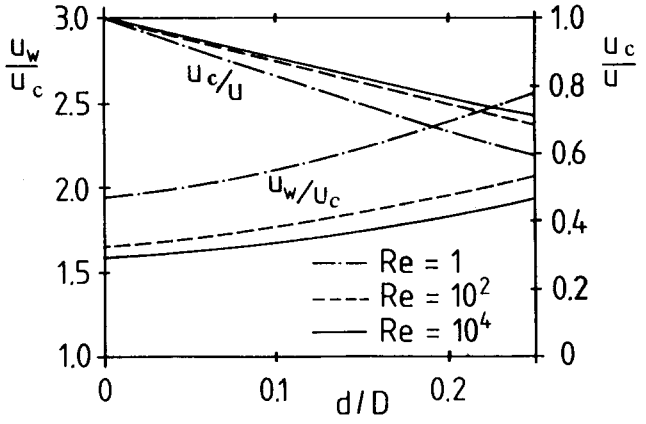

Figure 12. Ratio of wall-to-center and center-to-mean velocities.

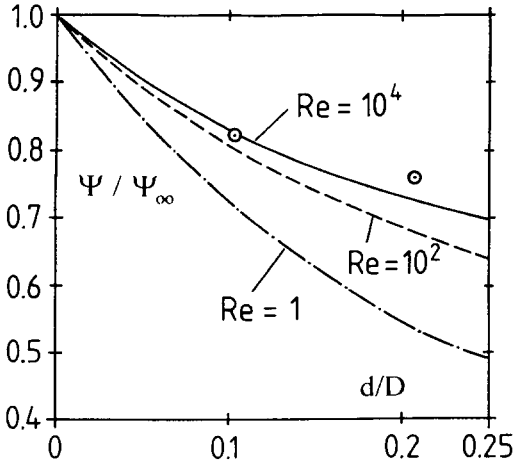

Figure 13. Effect of bypass flow on the pressure drop coefficient. (⊙) Present experimental result. Re = 10^4.

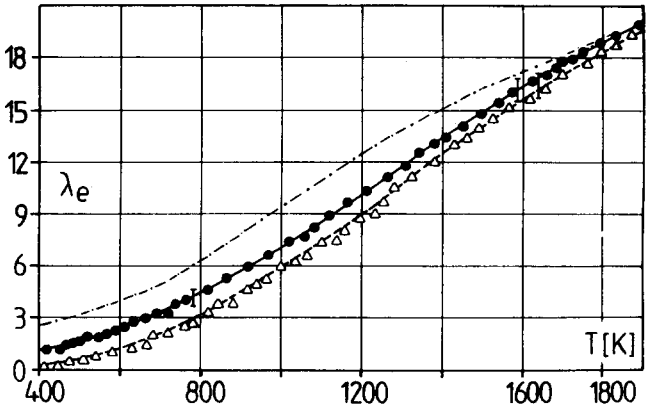

Figure 14. Effective conductivity of packed beds in vacuum and helium. Experiments and theory after Ref. 33; —·— 22.

and occurs as the boundary condition

$$-\lambda_e \left.\frac{\partial \vartheta}{\partial r}\right|_w = \alpha_w \Delta\vartheta \tag{32}$$

in the energy equation to be solved for the problem using the effective conductivity, λ_e, in the diffusion term.

The wall Nusselt number,

$$\mathrm{Nu}_w = \frac{\alpha_w d}{\lambda_g} = f(\mathrm{Re}, \mathrm{Pr}), \tag{33}$$

has been determined experimentally by numerous authors. The paper by Hahn and Achenbach [34] gives a survey of the experimental work. Their experimental results obtained by the naphthalene mass transfer method range from $50 < \mathrm{Re} < 2 \times 10^4$ and fit satisfactorily to the relation recommended in [22],

$$\mathrm{Nu}_w = \left(1 - \frac{1}{D/d}\right)\mathrm{Re}^{0.61}\,\mathrm{Pr}^{1/3}. \tag{34}$$

Equation (34) loses its justification below Reynolds numbers of the order of Re = 100, since diffusion effects dominate the heat transfer in comparison to the convective contribution. In other words, the thickness of the wall boundary layer is of the order of the particle size, which has consequences for the boundary conditions at the wall. The temperature difference $\Delta\vartheta$ vanishes, which is equivalent to $\alpha_w \to \infty$. Thus the temperature profile across the bed can be calculated immediately up to the wall by means of the energy equation.

CONCLUSION

The heat transfer and pressure drop of packed beds have been considered. The state of the art is described, and equations for the prediction of the related phenomena are recommended.

In particular, the particle-to-gas convective heat transfer can be calculated from the set of equations reported in [1]. Some emphasis was given to effects that can cause considerable errors in determining the convective heat transfer experimentally. Those mechanisms are natural

convection, heat losses via contact points, and the bypass effect.

The pressure drop coefficient can be correlated according to [10] or [22] over the entire Reynolds number range of interest. My results for very high Reynolds numbers indicate that the pressure drop coefficient becomes independent of Re for $\mathrm{Re}/(1/\epsilon) > 10^5$. Furthermore, the essential influence of the void fraction and its distribution across the bed is addressed, and the importance of the bypass flow is pointed out.

The effective thermal conductivity of a particle bed for stagnant and streaming gas is most reliably predicted by the models of [25–28]. Additional experimental results are mentioned [33] in which the bed temperature was increased up to 1870 K.

Finally, the wall-to-bed heat transfer is considered. Here the equations of [22] are recommended.

NOMENCLATURE

- A geometry coefficient, dimensionless
- c_p specific heat, J/(kg K)
- d particle diameter, m
- D tube diameter, m
- Gr Grashof number ($= gd^3 \Delta\rho/\rho\nu^2$), dimensionless
- g gravity constant, $\mathrm{m/s^2}$
- H height of the packed bed, m
- K constant, turbulent Peclet number, dimensionless
- Nu Nusselt number ($= \alpha d/\lambda$), dimensionless
- n exponent of the Reynolds number, dimensionless
- Δp pressure difference, $\mathrm{N/m^2}$
- Pe Péclet number ($= ud\rho\, c_p/\lambda$), dimensionless
- q heat flux, $\mathrm{W/m^2}$
- r radial coordinate, m
- Ra Rayleigh number (= Gr Pr), dimensionless
- Re Reynolds number ($= ud/\nu$), dimensionless
- Sh Sherwood number ($= \beta d/\delta$), dimensionless
- T temperature, K
- u velocity, m/s
- V volume, $\mathrm{m^3}$

Greek Symbols

- α heat transfer coefficient, $\mathrm{W/(m^2K)}$
- β mass transfer coefficient, m/s
- δ diffusion coefficient, $\mathrm{m^2/s}$
- ϵ void fraction, dimensionless
- η fluid dynamic viscosity, kg/(s m)
- λ thermal conductivity, W/(m K)
- ν kinematic viscosity, $\mathrm{m^2/s}$
- ρ fluid density, $\mathrm{kg/m^3}$
- ψ pressure drop coefficient, dimensionless

Subscripts

- ax axial
- c central
- e effective
- g gas
- h hydraulic
- l laminar
- p pore
- r radial
- s solid
- sp sphere
- w wall
- ∞ infinite

REFERENCES

1. Gnielinski, V., Gleichungen zur Berechnung des Wärme- und Stoffaustausches in durchströmten ruhenden Kugelschüttungen bei mittleren und grossen Pecletzahlen, *Verfahrenstechnik* **12**(6), 63–366, 1978.
2. Zehner, P., and Schlünder, E.U., Experimentelle und theoretische Bestimmung der effektiven Wärmeleitfähigkeit durchströmter Kugelschüttungen bei mässigen und hohen Temperaturen, *VDI-Forschungsheft* **558**, 1973.
3. Kunii, D., and Suzuki, M., Particle-to-Fluid Heat and Mass Transfer in Packed Beds to Fine Particles, *Int. J. Heat Mass Transfer* **10**, 845–852, 1967.
4. Schlünder, E. U., Über den Mechanismus der Stoffübertragung in Kontaktapparaten, *Verfahrenstechnik* **10**(10), 645–650, 1976.
5. Martin, H., Low Peclet Number Particle-to-Fluid Heat and Mass Transfer in Packed Beds, *Chem. Eng. Sci.* **33**, 913–919, 1978.
6. Vortmeyer, D., Packed Bed Thermal Dispersion Models and Consistent Sets of Coefficients, *Chem. Eng. Process.* **26**, 263–268, 1989.
7. Tsotsas, E., On Mass Transfer, Dispersion and Macroscopical Flow Maldistribution in Packed Tubes, *Chem. Eng. Process.* **31**, 181–190, 1992.
8. Karabelas, A. J., Wegner, T. H., and Hanratty, T. J., Use of Asymptotic Relations to Correlate Mass Transfer Data in Packed Beds, *Chem. Eng. Sci.* **26**, 1753–1765, 1971.
9. Raithby, G. D., and Hollands, K. G. T., A General Method of Obtaining Approximate Solutions to Laminar and Turbulent Free Convection Problems, *Adv. Heat Transfer* **11**, 265–315, 1975.
10. Sicherheitstechnische Regel des Kerntechnischen Ausschusses, Auslegung der Reaktorkerne von gasgekühlten Hochtemperaturreaktoren, KTA 3102.3, 1981.
11. Benenati, R. F., and Brosilow, C. B., Void Fraction Distribution in Beds of Spheres, *AIChE J.* **8**(6), 233–236, 1962.
12. Goodling, J., and Vachon, R., Radial Porosity Distribution in Cylindrical Beds Packed with Spheres, *Powder Technol.* **35**, 23–29, 1983.
13. Ouchlyama, N., and Tanaka, T., Porosity Estimation for Random Packings of Spherical Particles, *Ind. Eng. Chem. Fundam.* **23**, 490–493, 1984.
14. Daszkowski, Th., Strömung, Stoff- und Wärmetransport in schüttungsgefüllten Rohrreaktoren, Dissertation, Techn. Univ. Stuttgart, 1991.
15. Roblee, L. H. S., Baird, R. M., and Tierney, J. W., Radial Porosity Variations in Packed Beds, *AIChE J.* **4**, 460–464, 1958.
16. Achenbach, E., and Müller, M., Lückengrad und Druckverlust einer Raschig-Ring-Füllkörperschüttung, Jül-Rep. 2090, 1986.
17. Ziolkowska, I., and Ziolkowski, D., Fluid Flow Inside Packed Beds, *Chem. Eng. Process.* **23**, 137–164, 1988.
18. Carman, P. C., Fluid Flow Through Granular Beds, *Trans. Inst. Chem. Eng.* **15**, 150–156, 1937.
19. Barthels, H., Druckverlust in Kugelschüttungen, *Brennstoff-Wärme-Kraft* **24**, 233–236, 1972.
20. Yagi, S., Kunii, D., and Endo, K., Heat Transfer in Packed Beds Through Which Water Is Flowing, *Int. J. Heat Mass Transfer* **7**, 333–339, 1964.

21. Schlünder, E. U., Wärme- und Stoffübertragung zwischen durchströmten Schüttungen und darin eingebetteten Einzelkörpern, *Chem. Ing. Techn.* **38**, 767–979, 1966.
22. VDI-Wärmeatlas: Berechnungsbl. für d. Wärmeübergang/hrsgg. vom Verein Deutscher Ingenieure, VDI-gesellschaft Verfahrenstechnik und Chemieingenieurwesen. VDI-Verlag, Düsseldorf, 6. Aufl. 1991.
23. Tsotsas, E., and Martin, H., Thermal Conductivity of Packed Beds: A Review, *Chem. Eng. Process.* **22**, 19–37, 1987.
24. Tsotsas, E., Über die Wärme- und Stoffübertragung in durchströmten Festbetten: Experimente, Modelle, Theorien, *Fortsch.-Ber. VDI*, Reihe 3, Nr. 233, Düsseldorf, VDI-Verlag, 1990.
25. Zehner, P., and Schlünder, E. U., Wärmeleitfähigkeit von Schüttungen bei mässigen Temperaturen, *Chem.-Ing. Techn.* **42**, 933–941, 1970.
26. Zehner, P., and Schlünder, E. U., Einfluss der Wärmestrahlung und des Druckes auf den Wärmetransport in nicht durchströmten Schüttungen, *Chem.-Ing. Techn.* **44**, 1303–1308, 1972.
27. Bauer, R., and Schlünder, E. U., Die effektive Wärmeleitfähigkeit gasdurchströmter Schüttungen, *Vt-Verfahrenstechnik* **11**, 605–614, 1977.
28. Bauer, R., and Schlünder, E. U., Effective Radial Thermal Conductivity of Packings in Gas Flow, *Int. Chem. Eng.* **18**, 181–204, 1978.
29. Dalle Donne, M., and Sordon, G., Heat Transfer in Pebble Beds for Fusion Blankets, *Fusion Technol.* **17**, 597–635, 1990.
30. Okazaki, M., Yamasyki, T., and Gotoh, S., Effective Thermal Conductivities for Granular Beds of Various Binary Mixtures, *J. Chem. Eng. Jpn.* **14**, 183–189, 1981.
31. Botterill, J. S. M., Salway A. G., and Teoman, Y., The Effective Thermal Conductivity of High Temperature Particulate Beds. I. Experimental Determination, *Int. J. Heat Mass Transfer* **32**(3), 585–593, 1989.
32. Botteril, J. S. M., Salway, A. G., and Teoman, Y., The Effective Thermal Conductivity of High Temperature Particulate Beds. II. Model Predictions and the Implication of the Experimental Values, *Int. J. Heat Mass Transfer* **32**(3), 595–609, 1989.
33. Robold, K., Wärmetransport im Innern und in der Randzone von Kugelschüttungen, Diss. RWTH, Aachen, 1982.
34. Hahn, W., and Achenbach, E., Bestimmung des Wandwärmeübergangskoeffizienten von durchströmten Kugelschüttungen, Jül-Rep. 2093, 1986.

Received January 3, 1994; revised August 22, 1994